



Introduction of a Recyclable Basic Ionic Solvent with Bis-(NHC) Ligand Property and The Possibility of Immobilization on Magnetite for Ligand- and Base-Free Pd-Catalyzed Heck, Suzuki and Sonogashira Cross-Coupling Reactions in Water

Qingwang Min¹ · Penghua Miao¹ · Deyu Chu¹ · Jinghan Liu¹ · Meijuan Qi¹ · Milad Kazemnejadi²

Received: 7 December 2020 / Accepted: 23 January 2021

© The Author(s), under exclusive licence to Springer Science+Business Media, LLC part of Springer Nature 2021

Abstract

A new versatile and recyclable NHC ligand precursor has been developed with ligand, base, and solvent functionalities for the efficient Pd-catalyzed Heck, Suzuki and Sonogashira cross-coupling reactions under mild conditions. Furthermore, NHC ligand precursor was immobilized on magnetite and its catalytic activity was also evaluated towards the coupling reactions as a heterogeneous catalyst. The NHC ligand precursor was prepared with imidazolium functionalization of TCT followed by a simple ion exchange by hydroxide ions. However, the results revealed an excellent catalytic activity for the both homogeneous and heterogeneous catalytic systems. $1.52 \text{ g}\cdot\text{cm}^{-3}$ and 1194 cP was obtained for the density and viscosity of the NHC ligand precursor respectively. On the other hand, the heterogeneous type could be readily recovered from the reaction mixture and reused for several times while preserving its properties. Heterogeneous nature of the magnetic catalyst was studied by hot filtration, mercury poisoning, and three-phase tests. High to excellent yields were obtained for all entries for the both homogeneous and heterogeneous catalysts, which reflects the high consistency of the catalyst.

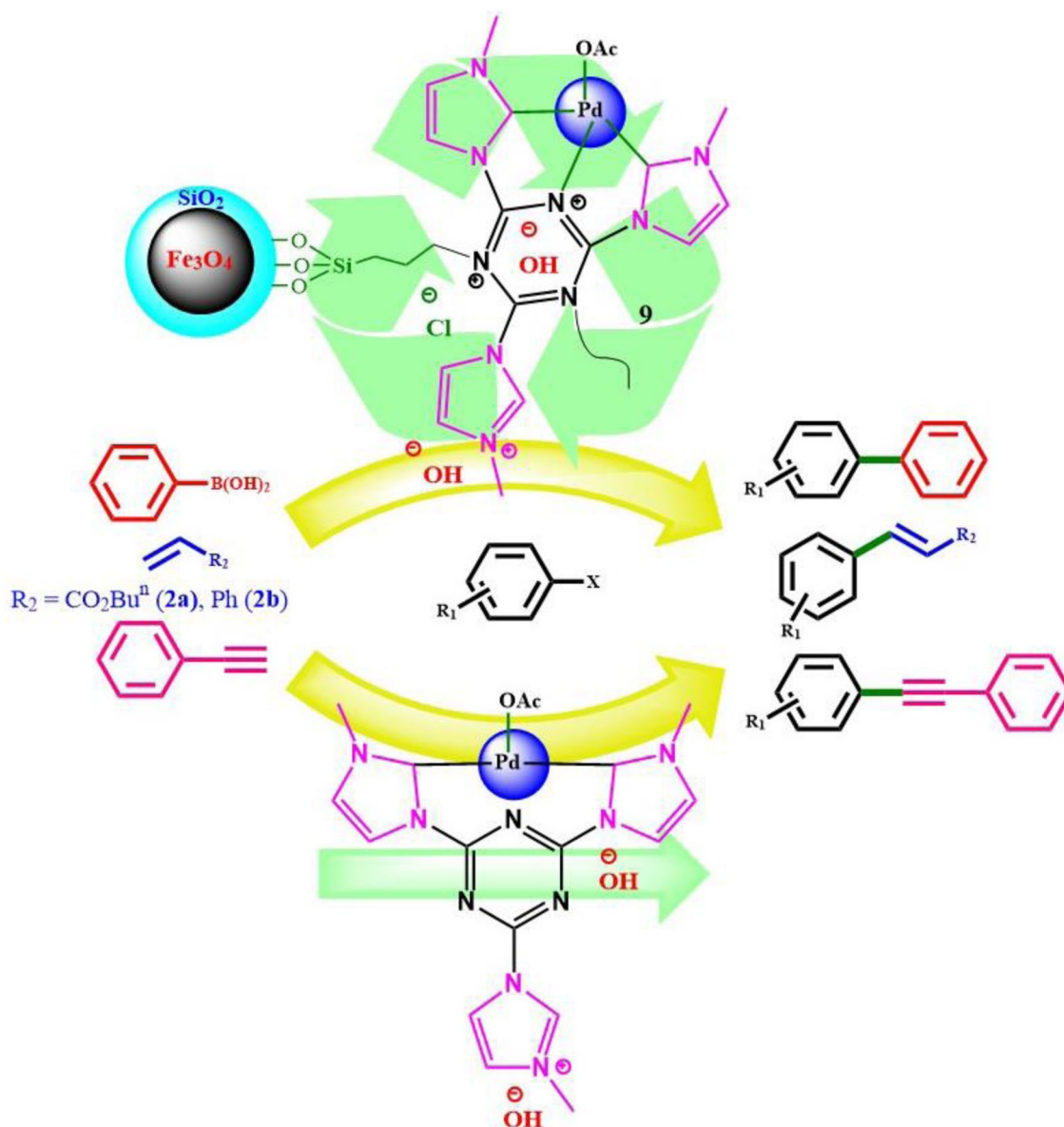
✉ Qingwang Min
minqw@dlpu.edu.cn

✉ Milad Kazemnejadi
miladkazemnejad@yahoo.com

¹ School of Light Industry and Chemical Engineering, Dalian Polytechnic University, Dalian 116034, PR China

² Department of Chemistry, College of Science, Shiraz University, 7194684795 Shiraz, Iran

Graphic Abstract



Keywords NHC ligand precursor · Homogeneous catalyst · Bis(nhc)pd complex · Ligand- · base · solvent-free · C–C cross-coupling reactions

1 Introduction

Pd-catalyzed C–C cross-coupling reactions comprise one of the most efficient and well-known methods for the of C–C bond formation [1]. Powerful palladium-based catalysts have enabled scientists to prepare various important and vital compounds by C–C bond formation that were previously unavailable or require several tedious steps [2]. Thus, cross-coupling reactions play a vital role in the synthesis of

organic compounds, agrochemical, pharmaceutical, and fine chemical industries [1].

There are seven main Pd-catalyzed C–C cross-coupling reactions including: Negishi, Suzuki–Miyaura, Stille, Sonogashira, Heck–Mizoroki, Kumada, and Heck–Matsuda reactions [2, 3].

The reaction between a halide or pseudo-halide and boronic acids, boronate esters or organoboranes compound for the assembly of biphenyl motifs catalyzed by the transition metal

is well known as Suzuki–Miyaura cross-coupling reaction [4]. Application in the synthesis of D159687 (an enzyme related to inflammatory and respiratory diseases) [5] and inhibitors of p38 mitogen-activated protein (MAP) kinases [6], are some examples for the application of Suzuki coupling reaction.

The Heck reaction is the Pd-catalyzed C–C cross-coupling reaction between aryl, and alkenes, or vinyl halides (or triflates) to give substituted alkenes [7]. It has widespread application in pharmaceutical in both industrial and Lab-scale syntheses [2, 8]. One example is its application in the preparation of Idebenone, a compound similar to coenzyme Q-10 used for Alzheimer's disease, Huntington's disease, liver disease, and heart disease [9]. Ginkgolic acid [10], anti-histaminic drug olopatadine [11], caffeine-styryl compounds [12], and vascular endothelial growth factor (VEGF) inhibitor axitinib [13] are some of the application of Heck reaction in the preparation of biological molecules.

Another important type of C–C cross-coupling reaction is coupling of Csp–Csp² between terminal acetylenic substrates with a vinyl, aryl halide or triflates catalyzed by Pd along with Cu as a co-catalyst for mainly construction of aryl acetylenes is known as Sonogashira reaction [14]. Sonogashira reaction has also a vital application in synthetic organic chemistry, in the formation of pharmaceutical and complex biological compounds from simple precursors [14, 15], and in the construction of olopatadine hydrochloride [11] and GRN-529 (a highly selective mGluR5 negative allosteric modulator) molecules [16]. Traditionally, it was catalyzed by a Pd catalyst along with a Cu as a co-catalyst. However, the presence of Cu persuades the by-product of Glaser-type homo-coupling between two terminal acetylenes [14]. Thus, the efforts conducted toward the development of copper-free methodologies.

In addition, coupling reactions have a special place in the synthesis of organic compounds. For example, direct sp³ arylation of 7-chloro-5-methyl-[1,2,4]triazolo[1,5-*a*]pyrimidine [17], enantioselective dicarbofunctionalization of unactivated alkenes [18], desulfonative cross-coupling of benzylic sulfone derivatives with 1,3-oxazoles [19], and cross-coupling reactions promoted by biaryl phosphorinane ligands [20] are some of the recent application of Pd-catalyzed cross-coupling reactions in organic synthesis.

Traditionally, these reactions catalyzed by a Pd salt in the presence of toxic and expensive phosphine ligand and Cu co-catalyst (in the case of Sonogashira coupling), that lack of catalyst recovery, unwilling by-products, toxic solvents disadvantages, limited its widespread application [1]. In this way, and note to their vital application in industry and medicine, numerous methodologies have been developed and reported for construction of various types of Pd-catalyzed C–C cross-coupling reactions, that can be point to: (1) Pd/GO/Fe₃O₄/PAMPS (GO = graphene oxide, PAMPS = poly 2-acrylamido-2-methyl-1-propanesulfonic acid) for Suzuki–Miyaura coupling reaction [4], (2) [Pd(1-tritylimidazole)₂Cl₂] complex

for Suzuki–Miyaura and Heck coupling reactions [7], (3) NiFe₂O₄@TABMA-Pd(0) (triazine bis[mercapto amine]) [21], (4) Pd@Hal-pDA-NPC (Hal = halloysite, pDA = poly-dopamine, NPC = *N*-doped porous carbon monolayer) [22], are some recent progresses for Pd-catalyzed C–C cross-coupling reactions. Moreover, Zahoor et al., reviewed development of green methodologies for Suzuki, Heck, Stille, and Chan–Lam cross-coupling reactions [3].

Palladium complexes of bis-*N*-heterocyclic carbene (NHC), have been successfully employed for a wide variety of organic reactions, especially cross-coupling reactions due to their strong σ -donor and weak π -acceptor properties [23]. Good catalytic activity, well stability, functionality tolerance, ease of preparation with cheap and accessible materials, and ease of modification are some of the advantages of *N*-heterocyclic carbene (NHC) ligands, which make them as a promising ligand for Pd-based catalytic systems [24, 25]. The efficient application of Pd-NHC complexes has been well known in organometallic chemistry and catalysts, especially in the last decade. Various modifications have been reported for Pd-NHC complexes that could be point to some recently: (1) *N,N'*-bridged binuclear NHC palladium complex for Suzuki reaction [23], (2) 2-hydroxyethyl substituted *N*-coordinate-Pd(II)(NHC) for direct arylation reaction [26], (3) [(PDCR)Pd(MeCN)](PF₆)₂ for electrochemical activation of CO₂ [27], (4) SPIONs-bis(NHC)-palladium(II) for C–C cross-coupling reactions [24], and (5) bi-nuclear NHC–palladium(II) complexes for Suzuki–Miyaura cross-coupling reactions [25].

In this work, a NHC ligand precursor with high basicity has been developed with bis-NHC pincer ligand property. In this way, a homogeneous water soluble NHC ligand precursor consisting of a counter anion of hydroxyl anions and imidazole cations on a triazine framework was prepared and characterized. The basic NHC ligand precursor could play the role of a ligand through a bis-(NHC) moiety, effective solvent and base. Pd ions could be coordinated via a bis-NHC moiety of the NHC ligand precursor and used as an efficient catalyst for the C–C cross-coupling reactions. The prominent advantage of the NHC ligand precursor was its recyclability from the aqueous phase and reused for several runs with preservation of its properties. Moreover, the NHC ligand precursor could be immobilized on magnetite and used as a heterogeneous magnetically recyclable nanocatalyst for the C–C cross-coupling reactions. The heterogeneous catalyst could be recycled for several consecutive runs with an insignificant reactivity loss.

2 Experimental

2.1 Materials and Instruments

All the chemicals were obtained from Sigma Aldrich or Merck companies and used as received without

further purification. Wang resin, polymer-bound 4-iodobenzene, was purchased from NovaBiochem containing 0.64–1.1 mmol g⁻¹ loading, 100–300 mesh, and cross-linked with 1% divinylbenzene used for three-phase test. All solvents were distilled (under Ar atmosphere) before use. All other reagents were of analytical grade. Progress of the coupling reactions were monitored by thin layer chromatography (TLC) on silica gel or gas chromatography (GC) on a Shimadzu-14B gas chromatograph with N₂ flow as a carrier gas and equipped with an HP-1 capillary column. Anisole was used as an internal standard for quantitative analyses. The viscosity of TAlm[OH] and TAlm[I] was obtained on a SMART L + PPR Fungilab instrument. FTIR analyses were recorded on a JASCO FT/IR 4600 spectrophotometer using KBr disk. The NMR spectra, ¹H (250 MHz) and ¹³C (62.9 MHz), were obtained using a Bruker Avance DPX-250 spectrometer in deuterated solvents of DMSO-*d*₆ or CDCl₃, and TMS as an internal standard. XPS analyses were conducted on a XR3E2 (VG Microtech) with anode X-ray source using Al-K α = 1486.6 eV. Energy-dispersive X-ray spectroscopy (EDX) analysis was conducted on a field emission scanning electron microscope, FESEM JOET 7600F, equipped with a spectrometer for energy dispersion of X-rays from Oxford instruments. The X-ray diffraction (XRD) studies of the nanoparticles were recorded on a Bruker AXS D8-advance X-ray diffractometer using Cu-K α radiation. Elemental analysis (C,H,N,S) was performed using a PerkinElmer-2004 apparatus. Transmission electron microscopy (TEM) images were taken on a Philips EM208 microscope operating at 100 kV. The size distribution of the nanoparticles was measured using the dynamic light scattering (DLS) method using a HORIBA-LB550 instrument. Field emission scanning electron microscopy (FE-SEM) image was taken on a MIRA3 TESCAN instrument. Thermogravimetric analysis (TGA) of the samples was performed using a NETZSCH STA 409 PC/PG under inert atmosphere (N₂) with a heating rate of 10 °C min⁻¹ in the temperature range of 25–850 °C. The magnetic behavior of the NPs was conducted on a Lake Shore vibrating sample magnetometer (VSM) at room temperature. ICP analyses were conducted on a VARIAN VISTA-PRO CCD simultaneous ICP-OES instrument.

2.2 Methods

2.2.1 Preparation of 1,1',1''-(1,3,5-Triazine-2,4,6-Triyl) Tris(3-Methyl-1H-Imidazol-3-ium) Iodide (TAlm[I]) (2)

At first, for the preparation of cyanuric iodide (1), 2, 4, 6-trichloro-1,3, 5-triazine (TCT, 0.37 g, 2.0 mmol) was added to 20 mL of dry acetone at room temperature. Then, NaI (1.5 g, 10 mmol) was added to the mixture. The flask was sealed and the mixture was stirred for 12 h. The color of

the solution was gradually turns into yellow. Then, 1-methylimidazole (15.0 mmol) was added to the mixture, then refluxed for 24 h. [TAlm]OH (2) was extracted to *n*-BuOH (3 × 10 mL). The resulting organic phases were placed in a vacuum oven (65 °C) for 24 h.

Characterization data for 2: Yellow oil, density: 2.22 g. cm⁻³, ¹H-NMR (250 MHz, D₂O) δ (ppm): 4.50 (s, 9H, CH₃), 7.32 (d, 3H, J=6.25 Hz, Im-H), 1.96 (d, 3H, J=6.25 Hz, Im-H), 8.98 (s, 3H, Im-H); ¹³C-NMR (62.9 MHz, D₂O) δ (ppm): 38.0, 117.7, 126.2, 144.6; EDX (%wt, average of five points) = C 26.55, N 18.88, I 44.57.

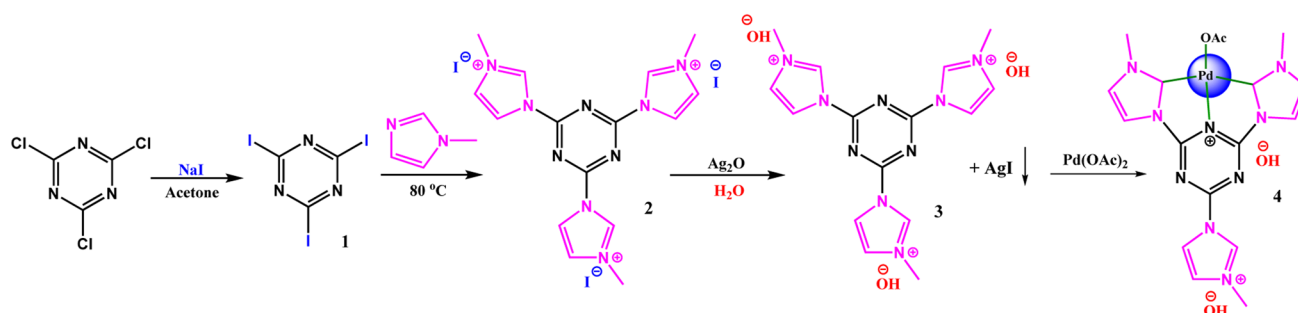
2.2.2 Preparation of 1,1',1''-(1,3,5-Triazine-2,4,6-Triyl) Tris(3-Methyl-1H-Imidazol-3-ium) Hydroxide (TAlm[OH]) (3)

Exchange of iodide counter ions with hydroxide was performed via a simple ion exchange using Ag₂O (as a part of Hofmann elimination). Ag₂O was also prepared in this study according to a simple procedure described elsewhere [28]. [TAlm]OH (2, 1.0 mL) was added to 20 mL of distilled water, then Ag₂O (8.0 mmol, 1.8 g) was added to the mixture in one step. The reaction was performed under reflux conditions for 8 h. The sediment (AgI) was filtered and the product was extracted to *n*-BuOH (3 × 10 mL). The resulting organic phases were dried in a vacuum oven (65 °C). Scheme 1 shows a schematic view for the preparation of [TAlm]OH.

Characterization data for 3: Yellow oil, ¹H-NMR (250 MHz, D₂O) δ (ppm): 4.14 (s, 9H, CH₃), 7.86 (d, 3H, J=7.00 Hz, Im-H), 8.10 (d, 3H, J=7.00 Hz, Im-H), 8.98 (s, 3H, Im-H); ¹³C-NMR (62.9 MHz, D₂O) δ (ppm): 38.7, 118.8, 126.6, 145.6; EDX (%wt) = C 49.33, N 35.76, O 14.91.

2.2.3 Determination of Hydroxyl Group in TAlm[OH]

The hydroxyl content in TAlm[OH] was measured by an acid titration assay. In this test, 1.0 mL of the NHC ligand precursor 3 was added to 50 mL of distilled water and stirred vigorously for 10 min (pH = 13.88). The resulting solutions was titrated with acetic acid 1.0 M in the presence of phenolphthalein indicator at room temperature under air conditions. About 11.96 mL acetic acid was consumed at the end point (pH = 7.0). At the same time, a blank was also titrated and the total volume of acetic acid was recorded. Based on the experiment, 1.0 mL of NHC ligand precursor contain 12.0 mmol hydroxyl group. So, with assumption of three equivalent of ⁻OH ions in a mmol of TAlm[OH], there are 4 mmol TAlm[OH] in a 1.0 mL of NHC ligand precursor. Based on the Mw of the NHC ligand precursor, it can be concluded that the density is equal to 1.55 g.cm⁻³.



Scheme 1 The preparation of TAlm[OH] (**3**) and TAlm[OH]-Pd (**4**)

2.2.4 Preparation of $\text{Fe}_3\text{O}_4@\text{SiO}_2$ -TAlm[OH]-Pd

$\text{Fe}_3\text{O}_4@\text{SiO}_2\text{Cl}$ was prepared through three steps according to a procedure described elsewhere [8, 29]. Next, complex **4** was prepared with dissolution of $\text{Pd}(\text{OAc})_2$ (1.0 mmol) to 5.0 mL EtOH, then, TAlm[OH] (3.0 mmol, 0.73 mL) was added to the mixture and stirred for 4 h at room temperature. The solid was filtered, washed with warm EtOH and deionized water, dried into oven and stored as a gray powder. TAlm[OH]-Pd was immobilized on $\text{Fe}_3\text{O}_4@\text{SiO}_2$ in one step as follows: $\text{Fe}_3\text{O}_4@\text{SiO}_2\text{Cl}$ (100 mg) was sonicated in 20 mL toluene at room temperature for 20 min. Then, TAlm[OH]-Pd (10.0 mg) was added to the mixture and refluxed for 24 h under N_2 atmosphere. Then, the mixture was allowed to cooled to room temperature, and the product was separated by applying an external magnetic field, washed with

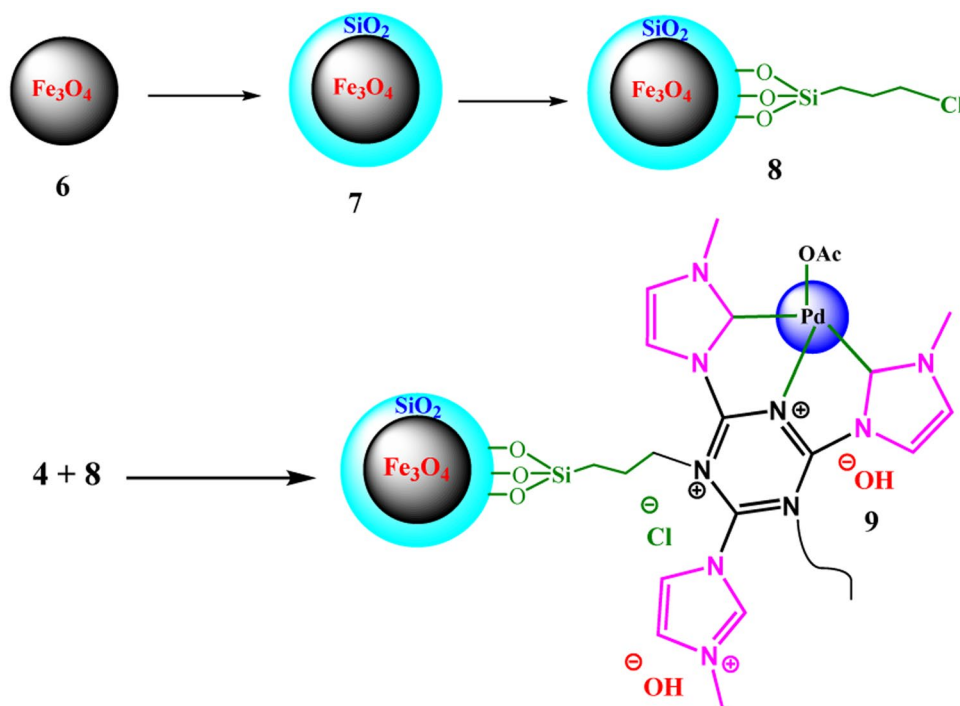
deionized water and EtOH (respectively), and dried into oven (60 °C) overnight (Scheme 2).

Characterization data for 4: $^1\text{H-NMR}$ (400 MHz, CDCl_3) δ (ppm): 3.04 (s, 6H, CH_3), 4.00 (s, 3H, CH_3), 6.67–6.69 (m, 2H), 6.93–6.95 (m, 2H), 7.46 (s, 2H), 7.67–7.68 (m, 2H), 8.63 (s, 1H); $^{13}\text{C-NMR}$ (100 MHz, CDCl_3) δ (ppm): 24.8, 36.4, 41.7, 112.8, 114.9, 121.4, 137.6, 162.3, 166.2, 170.2, 173.2; EDX (%wt, average of five points) = C 40.12, N 25.06, O 13.22, Pd 21.57.

2.2.5 General Procedure for Heck Cross-Coupling Reactions Catalyzed by $\text{Fe}_3\text{O}_4@\text{SiO}_2$ -TAlm[OH]-Pd and $\text{Pd}(\text{OAc})_2/\text{TAlm[OH]}$

2.2.5.1 Method 1 (Heterogeneous Catalyst) In a sealed tube equipped with a magnetic stirrer, aryl halide (1.0 mmol), alkene (1.3 mmol), and catalyst **9** (0.01 g, 0.2 mol% Pd)

Scheme 2 Preparation of $\text{Fe}_3\text{O}_4@\text{SiO}_2$ -TAlm[OH]-Pd



were mixed/dissolved in H₂O (2.0 mL). The mixture was refluxed for appropriate time which monitored by TLC (eluent: *n*-hexane/ ethyl acetate, 4:1). Upon reaction completion, the mixture allowed to cooled to room temperature, then, DCM (15.0 mL) was added to the mixture. The catalyst was separated magnetically, and the organic phase was separated, washed with deionized water (3×10 mL), and dried over Na₂SO₄. Finally, the solvent was evaporated under reduced pressure, and the product was purified and isolated by flash chromatography or a short column of silica gel to give the corresponding pure coupling product.

2.2.5.2 Method 2 (Homogeneous Catalyst) In a sealed tube equipped with a magnetic stirrer, aryl halide (1.0 mmol), alkene (1.3 mmol), and Pd(OAc)₂ (1.0 mol%) were mixed and dissolved in TAIM[OH] (2.0 mL). The mixture was refluxed for the appropriate time which monitored by TLC (eluent: *n*-hexane/ ethyl acetate, 4:1). After the completion of the reaction, 10 mL of water and 10 mL of CH₂Cl₂ was added to the mixture. The aqueous phase was further extracted with another 10 mL CH₂Cl₂. The organic phase was dried over MgSO₄, and the resulting coupling product was obtained after removal of the solvent under reduced pressure followed by flash chromatography.

The Suzuki and Sonogashira cross-coupling reactions were accomplished with a same procedure described for Heck reaction. Phenylboronic acid (1.0 mmol) and phenyl acetylene (1.0 mmol) was used for Suzuki and Sonogashira cross-coupling reactions respectively. TAIM[OH] could be extracted by two effective approaches: (i) removal of water under reduced pressure from the residue of aqueous phase; and (ii) extraction by pure *n*-BuOH (3×6 mL) and then, removal of *n*-BuOH under reduced pressure. However, in the present study, the first approach was served for the recycling of TAIM[OH]. The properties of TAIM[OH] was studied in each cycle by FTIR, elemental EDX analyses and viscose meter before use.

3 Results and Discussion

3.1 Catalyst Characterization

According to the acid titration assay, there is 12.0 mmol hydroxyl group in 1.0 ml of the imidazolium ionic compound. This gives a density equal to 1.55 g.cm⁻³ for the NHC ligand precursor **3**, which is completely in agreement with the measured density by a standard instrument (1.52 g.cm⁻³). Also, the viscosity of TAIM[OH] was found to be 1194 cP. Table 1 shows the general physical properties of TAIM[OH]. FTIR, ¹H-NMR, ¹³C-NMR and EDX analyses were completely confirmed the chemical structures of **2–4** compounds (ESI, Figs. S1–S4, and Scheme 1), which all

three Cl sites in TCT were functionalized with iodide in **2**, and subsequently with methyl imidazole in **3**. In addition, the complete elimination of iodide in the EDX spectrum of **3**, confirmed the successfully ion exchange reaction. Scheme 3 shows a mechanistic view for this transformation, where iodide counter ion attack to Ag₂O to give TAIM[OAg] intermediate. Then, in the presence of a water molecule, AgOH is formed and provides the desire product. Another prove for this process, was the formation of AgI sediments, which characterized by FTIR analysis. It worth noted that the reaction was failed with TCT and didn't found any product for **4** (Scheme 1). This could be directly related to the difference of atomic radius of Cl (175 pm) and iodide (198 pm), wherein iodine binds more weakly to the imidazolium cation than chlorine. However, with cyanuric iodide, the reaction processed efficiently.

X-ray diffraction patterns of Fe₃O₄, Fe₃O₄@SiO₂, and Fe₃O₄@SiO₂-TAIM[OH]-Pd is shown in Fig. 1. Surface functionalization of magnetite with silica shell don't change the crystal structure of Fe₃O₄ NPs, however, the peaks intensity and sharpness decreased slightly and an amorphous peak at 2θ = 13.1° indicate the presence of amorphous silica shell coated on magnetite in agreement with the literature (Fig. 1a,b) [2, 8]. Further functionalization of Fe₃O₄@SiO₂ with TAIM[OH]-Pd causes to more reduction in peaks intensity slightly (Fig. 1c). However, no change in the pattern and the peaks position, confirmed that the crystal structure of Fe₃O₄ remain intact during functionalization (Fig. 1c). A newly formed peak at 2θ = 9.1° indicating a synergetic effect between amorphous silica shell and TAIM[OH]-Pd, which shifted the amorphous peak to the lower degrees, consistence with the literature [30]. This shift is a prove for the further successful functionalization of Fe₃O₄@SiO₂ with TAIM[OH]-Pd complex.

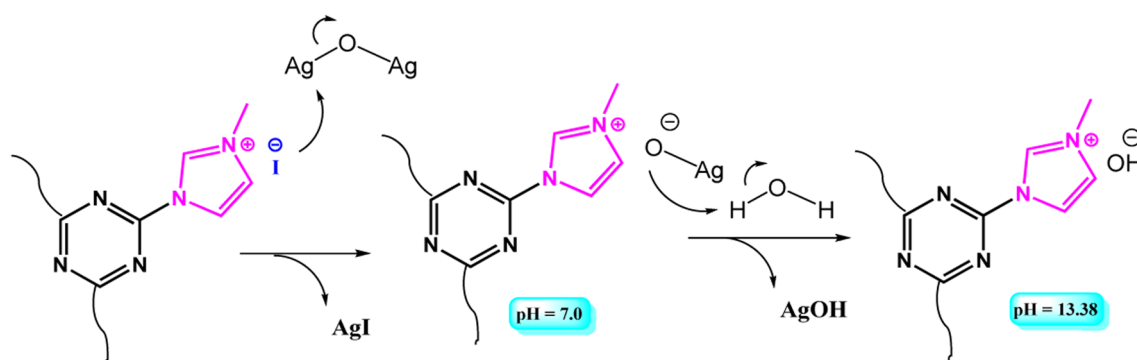
From the TEM image of Fe₃O₄@SiO₂-TAIM[OH]-Pd nanoparticles, the particles are nearly spherical in shape with a homogeneous morphology and an average size of 30 nm (Fig. 2A). FE-SEM image of Fe₃O₄@SiO₂-TAIM[OH]-Pd showed a homogeneous morphology for the NPs in agreement with the TEM image (Fig. 2B). Also, the size distribution of the NPs was studied by DLS analysis. The results showed that the main of NPs have a size of between 25–27 nm, in agreement with the TEM image (Fig. 2C).

Magnetic behavior of the samples was studied by VSM analysis. The results represent a superparamagnetic behavior

Table 1 Physical properties of TAIM[OH] NHC ligand precursor

Physical properties	Mw (g.mol ⁻¹)	Color/appearance	Density (g.cm ⁻³)	Viscosity (cP)
Value	375.4	Yellow oil	1.52 ^a	1194

^aBased on apparatus. 1.55 g.cm⁻³ from the acid titration assay



Scheme 3 A mechanistic view for the ion exchange reaction (as a part of Hofmann elimination method) during the preparation of TAIm[OH] NHC ligand precursor

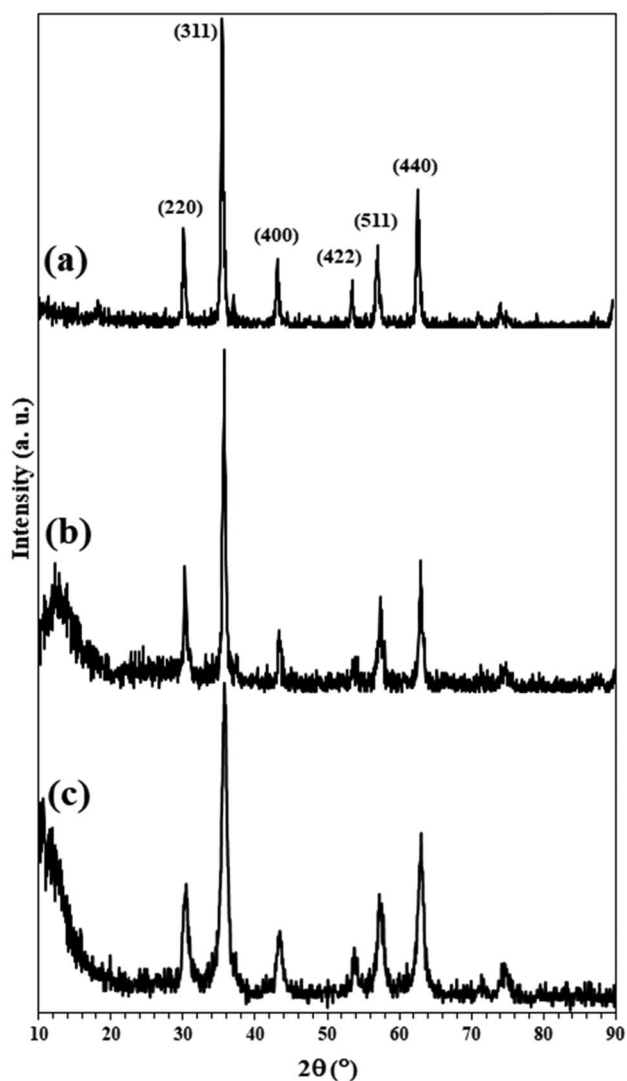


Fig. 1 XRD patterns of **a** Fe_3O_4 , **b** $\text{Fe}_3\text{O}_4@SiO_2$, and **c** $\text{Fe}_3\text{O}_4@SiO_2$ -TAIm[OH]-Pd

for Fe_3O_4 , $\text{Fe}_3\text{O}_4@SiO_2$ and catalyst **9**, with a zero coercivity for all of them (Fig. 2D). The saturation magnetization of 69, 40, and 20 emu g^{-1} was found for Fe_3O_4 , $\text{Fe}_3\text{O}_4@SiO_2$, and catalyst **9** respectively. This magnetization reduction in each step is directly related to the immobilization of a diamagnetic shell in each step, that dilute the applied magnetic field [8]. Although, a large decrease in magnetization was observed, however it is a strong confirmation for successful immobilization of magnetite with organic compounds (Fig. 2D-c). Despite this reduction, the catalyst could be collected from the reaction mixture less than 1.0 min completely.

To manifest and confirm the elements in the catalyst and oxidation state of Pd, an overall survey and high resolution XPS analysis was performed on the catalyst **9**. As shown in Fig. 3a, all expected elements were detected in their corresponding binding energies. An important point was the detection of small amount of Cl in the XPS spectrum of **9**, which was in agreement with the corresponding EDX analysis and the proposed structure sketched for **9** in Scheme 2 (Fig. 3a). The high resolution XPS 3d-Pd analysis confirmed the presence of both $\text{Pd}^{(0)}$ and $\text{Pd}^{(+2)}$ simultaneously in the catalyst. As shown in Fig. 3b, the peaks at 337.25 eV and 342.55 eV were assigned to the binding energies of $3d_{5/2}$ and $3d_{3/2}$, correspond to +2 oxidation state of Pd [31]. Also, two peaks with smaller intensity at 335.1 eV and 340.3 eV demonstrated that a small amount of Pd are in zero oxidation state [31, 32]. This was a positive point in a cross-coupling reaction with a possible oxidative-addition and reductive-elimination stages, that was seen for Pd catalyzed C–C cross-coupling reactions.

EDX analysis of the NPs confirmed the presence of all expected elements including C, N, O, Si, Fe, Pd, and Cl in agreement with the suggested structure for $\text{Fe}_3\text{O}_4@SiO_2$ -TAIm[OH]-Pd (Scheme 2, and Fig. 3c). More importantly, there is 2.08%wt Pd in the catalyst, that is completely

Fig. 2 **a** TEM image, **b** FE-SEM image, and **c** DLS of catalyst **9**. **d** VSM curves of **a** Fe_3O_4 , **b** $\text{Fe}_3\text{O}_4@/\text{SiO}_2$, and **c** catalyst **9**

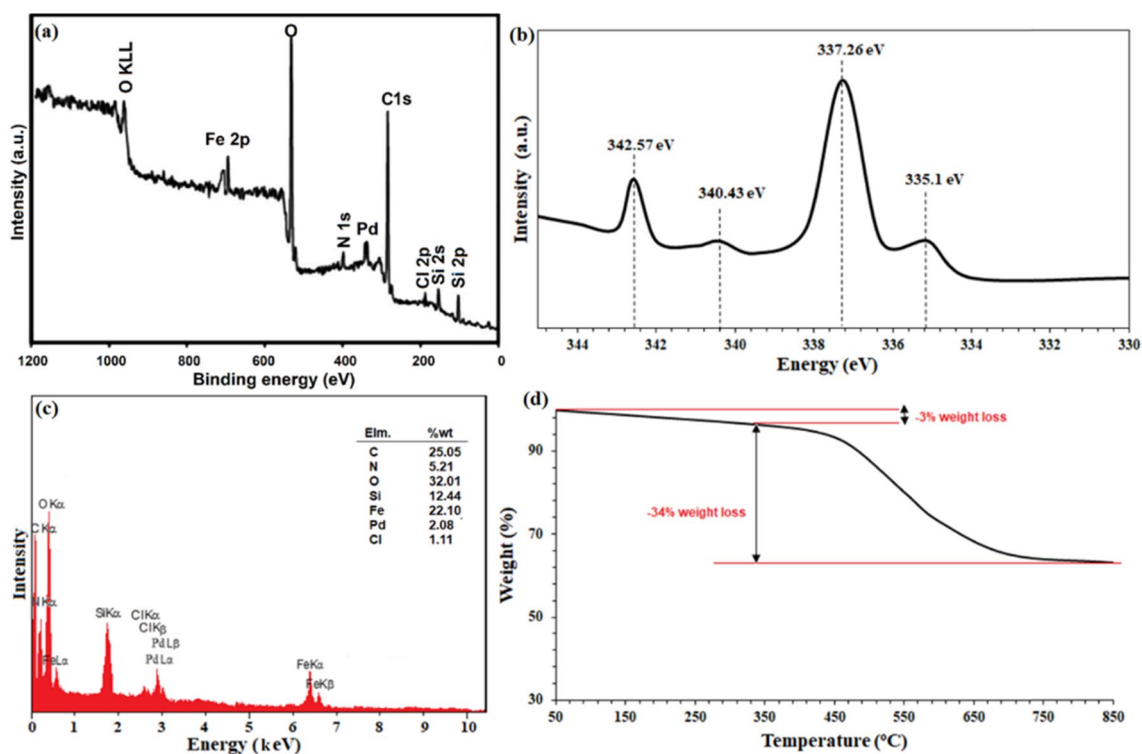
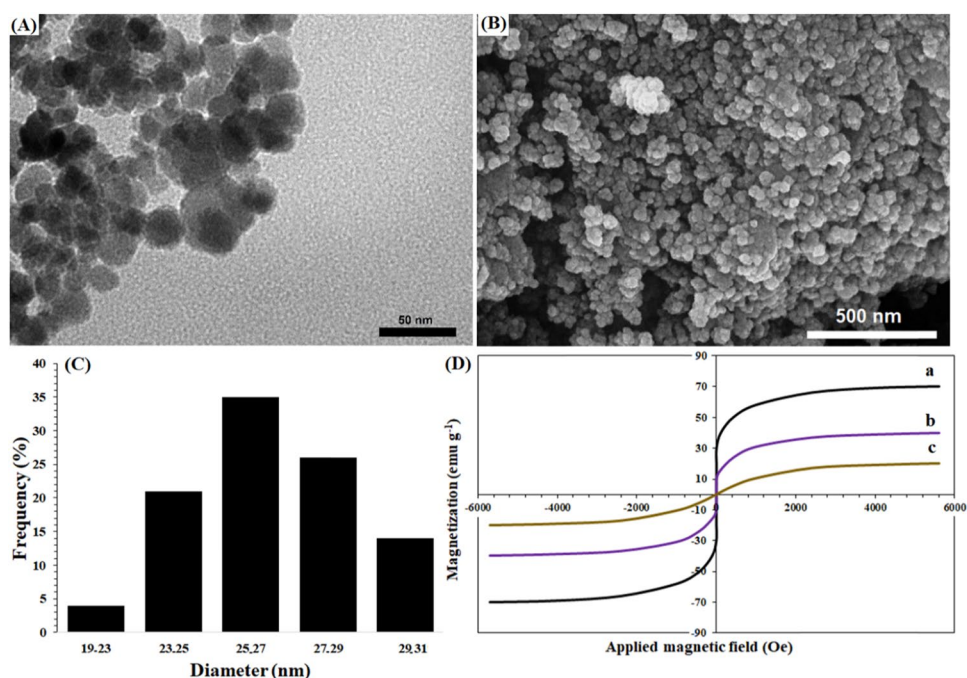


Fig. 3 **a** An overall survey and **b** high resolution (normalized, energy-corrected) XPS analysis, **c** EDX, and **d** TGA analyses of catalyst **9**

consistence with ICP analysis (2.12%wt). The percentage of all other elements has been shown in the inset table in Fig. 3c.

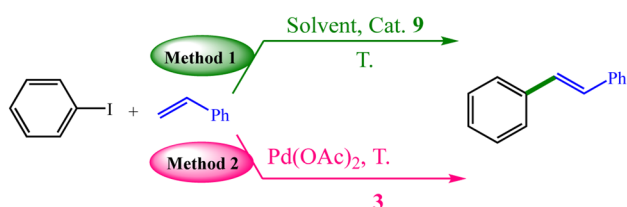
Thermal behavior of **9** was shown in Fig. 3d. The NPs demonstrated good thermal stability and there is a main

weight loss in the temperature span of 300–750 °C (starts at 300 °C with a gentle slope) with 34% weight loss. This weight loss could be directly related to the organic moieties (containing Pd complex) immobilized on magnetite, completely in agreement with the EDX analysis. Another small

weight loss occurs below 300 °C, that could be attributed to the adsorbed water molecule on the surface or trapped in the crystal structure of the NPs (Fig. 3d). Totally, 37% weight loss was observed until 850 °C, which suggest a good thermal stability for the NPs.

3.2 Optimization of Reaction Parameters

To find optimum conditions for the C–C cross-coupling reactions catalyzed by $\text{Fe}_3\text{O}_4@\text{SiO}_2\text{-TAIm}[\text{OH}]\text{-Pd}$ and $\text{TAIm}[\text{OH}]$, the reaction parameters such as solvent, temperature, and catalyst amount were studied. For this goal, the Heck coupling reaction of iodobenzene with styrene was chosen as a model reaction to study of the reaction



Scheme 4 The model cross-coupling reaction of iodobenzene with styrene for optimization of reaction parameters via method 1 and method 2 catalyzed by $\text{Fe}_3\text{O}_4@\text{SiO}_2\text{-TAIm}[\text{OH}]\text{-Pd}$ and $\text{Pd}(\text{OAc})_2/\text{TAIm}[\text{OH}]$ respectively

parameters for the both heterogeneous (Scheme 4, method 1) and homogeneous (Scheme 4, method 2) catalytic systems. It should be noted that the reactions were performed in the absence of any basic reagent.

Figure 4a shows the effect of solvent on method 2. The high efficiency of 86–88% was obtained for water, EtOH, MeOH, DMF, and DMSO solvents for 85 min. The low efficiency of 55% and 75% was obtained for CH_3CN and toluene respectively (Fig. 4a). It seems that the properties such as dielectric constant, polarity, and being protic for the solvents, provide better conditions for the coupling reaction. The reaction under solvent-free conditions didn't show any satisfactory results (30% for 85 min, 30% for 120 min, at 120 °C). Effect of temperature was evaluated in the next step for the both methods (Fig. 4b). Method 1 (using $\text{Fe}_3\text{O}_4@\text{SiO}_2\text{-TAIm}[\text{OH}]\text{-Pd}$) gave the high possible efficiency at reflux conditions. Decrease of temperature, decreases the efficiency linearly (Fig. 4b). On the other hand, for method 2 using $\text{TAIm}[\text{OH}]$, there is not any product at temperatures below 40 °C; and 120 °C was the premium temperature with 90% isolated yield (Fig. 4b). Raising temperature didn't effect on the reaction efficiency. Finally, the catalyst amount of 9 and $\text{Pd}(\text{OAc})_2$ was studied for methods 1 and 2 (Fig. 4c,d). According to ICP analysis, there is 2.12% wt Pd in the catalyst. So, based on amount of starting material for cross-coupling reactions, it could be concluded that the

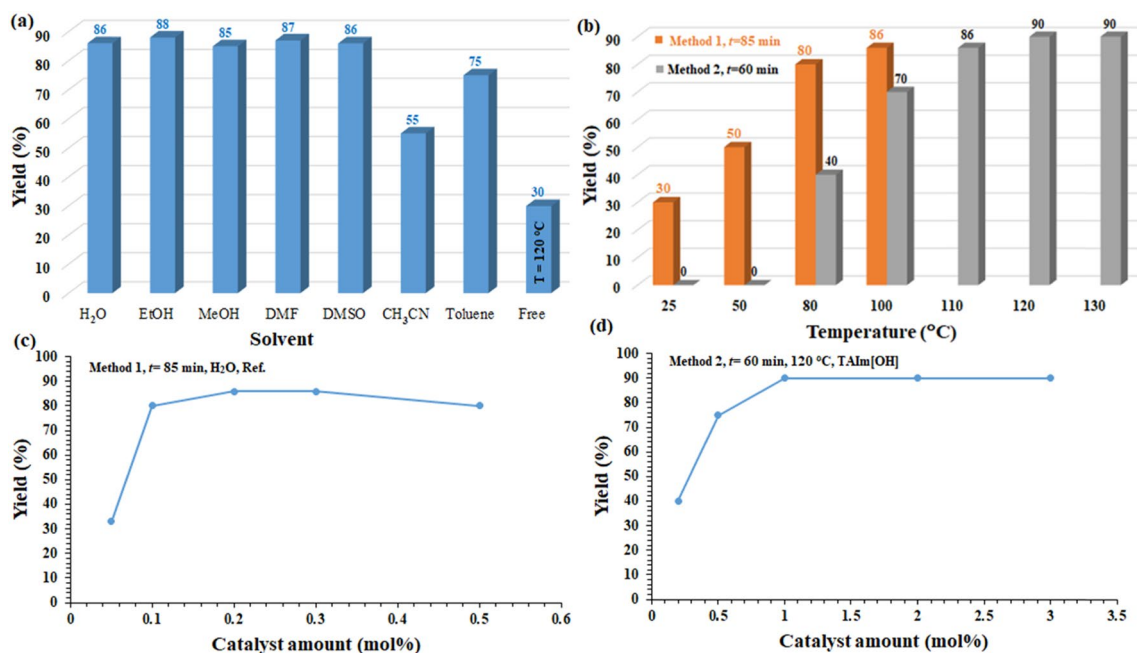
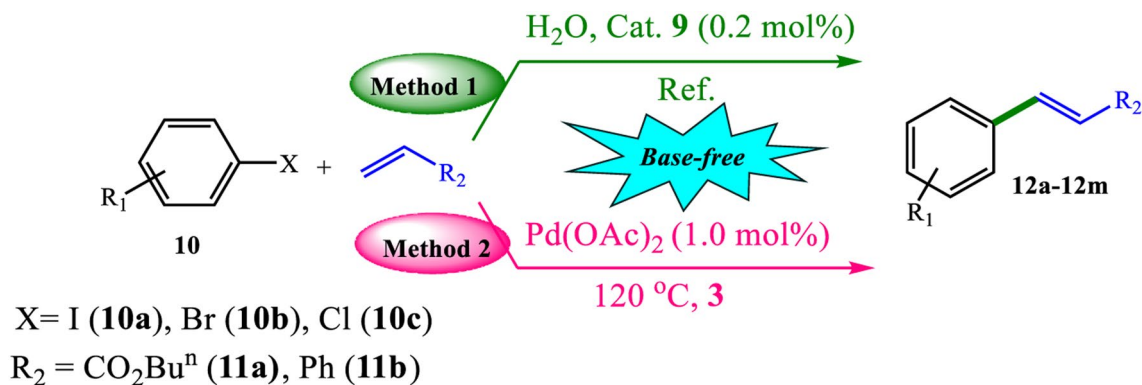


Fig. 4 a Solvent effect over the Heck cross-coupling reaction of iodobenzene with styrene via method 1. conditions: Solvent (2.0 mL, except the case of “free”), $\text{Fe}_3\text{O}_4@\text{SiO}_2\text{-TAIm}[\text{OH}]\text{-Pd}$ (as a catalyst), Reflux (except the case of “free”), 85 min. **b** Effect of temperature over the Heck cross-coupling reaction of iodobenzene with sty-

rene via method 1 and method 2 (85 min for method 1, and 60 min for method 2). Effect of **c** $\text{Fe}_3\text{O}_4@\text{SiO}_2\text{-TAIm}[\text{OH}]\text{-Pd}$ amount and **d** $\text{Pd}(\text{OAc})_2$ over the Heck cross-coupling reaction of iodobenzene with styrene via the method 1 and method 2, respectively (85 min, H₂O, Ref. for method 1, and 60 min, 120 °C for method 2)

reactions were catalyzed in the presence of 0.2 mol% Pd catalyst for method 1 (catalyst **9**) and 2 (Pd(OAc)₂) of Fe₃O₄@SiO₂-TAIm[OH]-Pd. The results demonstrated that 0.2 mol% and 1.0 mol% were the premium amounts of

Table 2 Heck cross-coupling reaction of aryl halides with alkenes catalyzed by Fe₃O₄@SiO₂-TAIm[OH]-Pd and Pd(OAc)₂/TAIm[OH]



Entry	X	R ₁	R ₂	Product	Time (min)		Yield (%)	
					Method 1	Method 2	Method 1	Method 2
1	I	H	Ph	12a	85	60	86	90
2	Br	H	Ph		100	80	82	86
3	Cl	H	Ph		250	220	70	75
4	I	4-MeO	Ph	12b	120	100	82	95
5	Br	4-MeO	Ph		135	110	74	90
6	Cl	4-MeO	Ph		300	280	60	75
7	I	4-NO ₂	Ph	12c	60	40	92	96
8	Br	4-NO ₂	Ph		77	55	84	90
9	Cl	4-NO ₂	Ph		200	175	80	84
10	I	4-CN	Ph	12d	60	45	90	98
11	Br	4-CN	Ph		70	60	85	95
12	Cl	4-CN	Ph		200	180	78	89
13	I	4-Me	Ph	12e	65	50	85	90
14	Br	4-Me	Ph		70	60	80	90
15	Cl	4-Me	Ph		220	200	70	82
16	I	4-Br	Ph	12f	75	55	90	95
17	Br	4-Cl	Ph	12g	90	75	80	84
18	I	H	CO ₂ ⁿ Bu	12h	95	65	85	94
19	Br	H	CO ₂ ⁿ Bu		120	80	80	85
20	Cl	H	CO ₂ ⁿ Bu		260	240	70	70
21	I	4-MeO	CO ₂ ⁿ Bu	12i	135	110	85	90
22	I	4-NO ₂	CO ₂ ⁿ Bu	12j	66	45	90	95
23	I	4-CN	CO ₂ ⁿ Bu	12k	60	55	88	95
24	I	4-OH	CO ₂ ⁿ Bu	12l	70	60	80	85
25	I	4-Br	CO ₂ ⁿ Bu	12m	80	60	90	90

Bold numbers represent the number of compounds (or products)

^aReaction conditions: Aryl halide (1.0 mmol), alkene (1.3 mmol), sealed tube

^bFor method 1: Fe₃O₄@SiO₂-TAIm[OH]-Pd (0.01 g, 0.2 mol% Pd), H₂O (2.0 mL), Ref

^cFor method 2: Pd(OAc)₂ (1.0 mol%), TAIm[OH] (2.0 mL), 120 °C

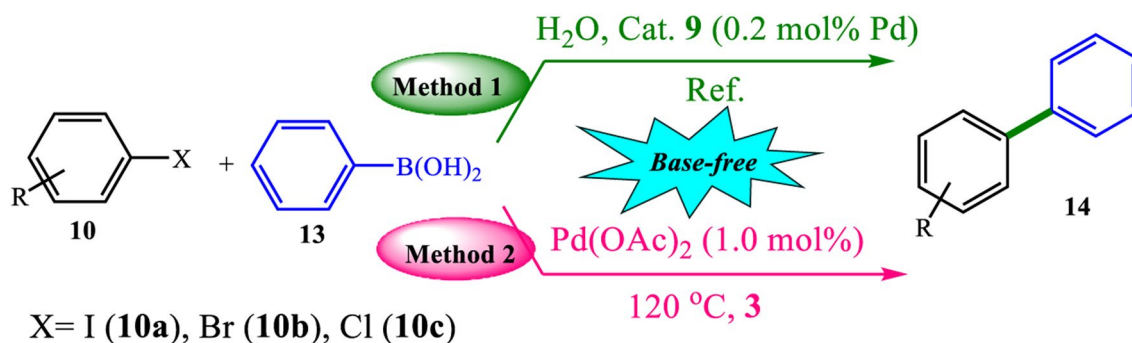
respectively. The relationship between catalyst amount mol% and reaction isolated yield was shown in Fig. 4c,d.

3.3 Catalytic Activity

The catalytic activity of $\text{Fe}_3\text{O}_4@\text{SiO}_2\text{-TAIm[OH]-Pd}$ and $\text{Pd(OAc)}_2/\text{TAIm[OH]}$ was studied as two heterogeneous and

homogeneous systems, respectively, for C–C cross-coupling reactions. It should be noted that for both systems, no base was used due to the basic intrinsic nature of the TAIm[OH] in the both catalytic systems. Table 2 shows the results of this study for the Heck reaction. As shown in the table, a wide range of substrates bearing electron donor and electron withdrawing substituent can be coupled with styrene and

Table 3 Suzuki cross-coupling reaction of aryl halides with phenylboronic acid catalyzed by $\text{Fe}_3\text{O}_4@\text{SiO}_2\text{-TAIm[OH]-Pd}$ and $\text{Pd(OAc)}_2/\text{TAIm[OH]}$



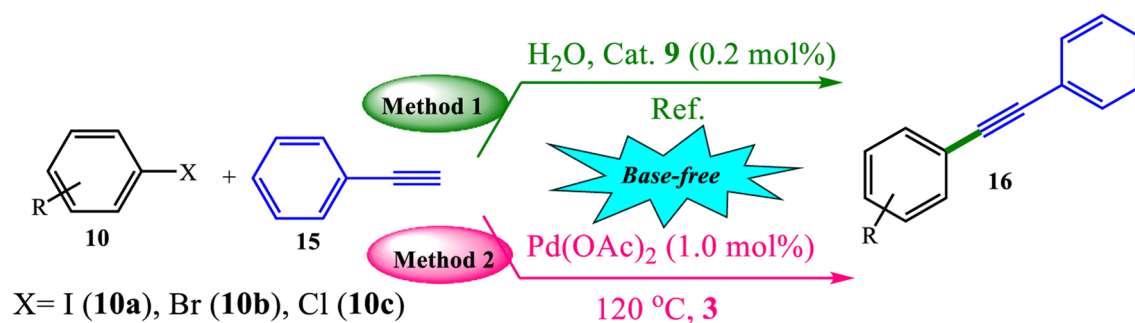
Entry	X	R	Product	Time (min)		Yield (%)	
				Method 1	Method 2	Method 1	Method 2
1	I	H	14a	35	30	96	96
2	Br	H		60	40	90	96
3	Cl	H		175	160	90	90
4	I	4-MeO	14b	60	50	84	90
5	Br	4-MeO		65	50	80	88
6	Cl	4-MeO		190	170	70	82
7	I	4-NO ₂	14c	33	25	95	98
8	Br	4-NO ₂		45	35	92	95
9	Cl	4-NO ₂		190	160	85	90
10	I	4-CN	14d	65	50	94	94
11	Br	4-CN		80	66	78	90
12	Cl	4-CN		225	185	68	82
13	I	4-Me	14e	80	70	85	88
14	Br	4-Me		110	95	75	90
15	Cl	4-Me		240	220	65	80
16	I	4-Br	14f	85	75	85	85
17	Br	4-Cl	14 g	120	100	70	80
18	I	1-Naphthyl	14 h	85	80	90	90
19	Br	1-Naphthyl		100	95	80	90
20	Cl	1-Naphthyl		245	220	70	78
21	I	2-Pyrimidyl	14i	95	90	95	95
22	Br	2-Pyrimidyl		115	110	84	90
23	Cl	2-Pyrimidyl		260	240	60	80

Bold numbers represent the number of compounds (or products)

^aReaction conditions: Aryl halide (1.0 mmol), phenylboronic acid (1.3 mmol), sealed tube

^bFor method 1: $\text{Fe}_3\text{O}_4@\text{SiO}_2\text{-TAIm[OH]-Pd}$ (0.01 g, 0.2 mol% Pd), H_2O (2.0 mL), Ref

^cFor method 2: Pd(OAc)_2 (1.0 mol%), TAIm[OH] (2.0 mL), 120 °C

Table 4 Sonogashira cross-coupling reaction of aryl halides with phenyl acetylene catalyzed by $\text{Fe}_3\text{O}_4@\text{SiO}_2\text{-TAIm[OH]-Pd}$ and $\text{Pd(OAc)}_2/\text{TAIm[OH]}$ 

Entry	X	R	Product	Time (min)		Yield (%)	
				Method 1	Method 2	Method 1	Method 2
1	I	H	16a	120	100	95	97
2	Br	H		180	145	90	94
3	Cl	H		200	160	84	90
4	I	4-MeO	16b	150	130	95	95
5	Br	4-MeO		210	170	88	92
6	Cl	4-MeO		230	200	80	84
7	I	4-NO ₂	16c	100	100	92	98
8	Br	4-NO ₂		165	150	88	94
9	Cl	4-NO ₂		190	175	80	90
10	I	4-CN	16d	120	110	96	96
11	Br	4-CN		190	175	90	95
12	Cl	4-CN		220	190	82	90
13	I	4-Me	16e	155	140	90	94
14	Br	4-Me		200	180	88	90
15	Cl	4-Me		240	210	82	85
16	I	4-Br	16f	150	140	92	96
17	Br	4-Cl	16 g	250	200	85	92
18	I	1-Naphthyl	16 h	190	180	90	92
19	Br	1-Naphthyl		135	120	95	95
20	Cl	1-Naphthyl		150	135	92	95
21	I	3-Pyrimidyl	16i	95	90	96	98
22	Br	3-Pyrimidyl		220	200	80	84
23	Cl	3-Pyrimidyl		180	180	80	80

Bold numbers represent the number of compounds (or products)

^aReaction conditions: Aryl halide (1.0 mmol), phenyl acetylene (1.3 mmol), sealed tube

^bFor method 1: $\text{Fe}_3\text{O}_4@\text{SiO}_2\text{-TAIm[OH]-Pd}$ (0.01 g, 0.2 mol% Pd), H_2O (2.0 mL), Ref

^cFor method 2: Pd(OAc)_2 (1.0 mol%), TAIm[OH] (2.0 mL), 120 °C

n-butyl acrylate alkenes. In general, the homogeneous system has better efficiency in terms of product yield (11–14% better efficiency) and time (20–25 min less time than the heterogeneous system) than the heterogeneous system using $\text{Fe}_3\text{O}_4@\text{SiO}_2\text{-TAIm[OH]-Pd}$.

Three other notable points from Table 2 are: (1) Aryl halides containing electron withdrawing groups such as 4-NO₂ and 4-CN provide better efficiency than aryl halides containing electron donor substituent such as 4-MeO and 4-Me (for example compare **12b** with **12c**, and **12i** with **12j**) completely in agreement with the reported Pd-catalyzed C–C

Table 5 Designed control experiments for cross-coupling reaction of iodobenzene with styrene through method 2

Entry	Catalyst	Base	Solvent	Time (min)	Yield (%)
1	TAIm[I] (2)/Pd(OAc) ₂	–	–	60	12
2	TAIm[I] (2)/Pd(OAc) ₂	K ₃ PO ₄ ^b	–	60	85
3	TAIm[I] (2)/Pd(OAc) ₂	K ₂ CO ₃ ^b	–	60	75
4	TAIm[OH] (3)/Pd(OAc) ₂	–	–	60	90
5	TAIm[OH] (3)/Pd(OAc) ₂	K ₃ PO ₄	–	60	90
6 ^c	Pd(OAc) ₂	–	DMF (or H ₂ O)	60	–
7 ^{d,e}	TAIm[OH]-Pd (4)	–	–	60	85

^aReaction conditions: Iodobenzene (1.0 mmol), styrene (1.3 mmol), Pd(OAc)₂ (1.0 mol%), TAIm[OH] (2.0 mL), Ref., sealed tube

^b2.0 mmol

^cPd(OAc)₂: 1.0 mol%, DMF/H₂O (2.0 mL)

^d0.01 mmol (5.2 mg)

^eThe efficiency reached to 90 for 65 min

cross-coupling reactions in literature [2, 7], (2) the reactivity of aryl halides as a leaving group was as order of: I > Br > Cl (Table 2) and (3) Styrene showed a higher activity for the coupling reaction than *n*-butyl acrylate in a completely same reaction conditions (for example, compare **12a** and **12h**). As will be shown in following, these results could be extended to Suzuki and Sonogashira suitably. Moreover, the results suggest a mechanism including oxidative-addition and reductive elimination for both catalytic systems.

Significant results for Heck reaction also led to the evaluation of catalyst capability for Suzuki and Sonogashira coupling reactions. The results for these reactions were also significant for both systems, and good to excellent efficiencies were achieved for all substrates. Tables 3 and 4 show the results of this study. Similar to the Heck reaction, aryl halides containing electron withdrawing groups provided better efficiency than the electron donor type for both Sonogashira and Suzuki reactions. The results of the homogeneous system showed that TAIm[OH] has multiple functions as a solvent, base and ligand and catalyzes the coupling reactions well, only in the presence of Pd (OAc)₂.

3.4 Control Experiments

In order to clarify the ligand and base role of TAIm[OH], several control reactions were performed over the Heck model reaction. Initially, compound **2** (2.0 mL) was used instead of **3** to the Heck model coupling reaction. Efficiency dropped to 12% for an hour (Table 5, entry 1).

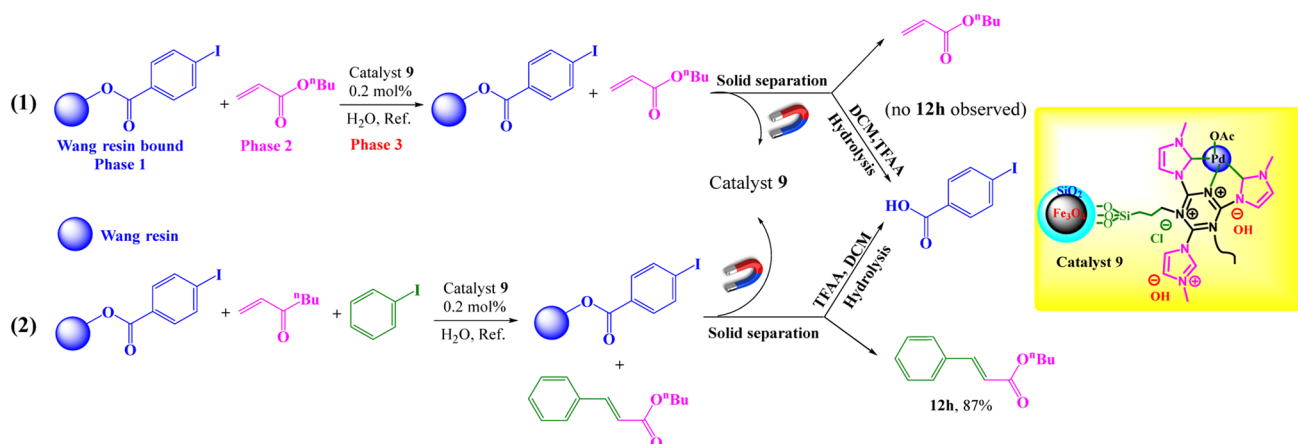
Another interesting point is that the efficiency in the presence of K₃PO₄ and K₂CO₃ bases created 85% and 75% efficiency for one hour at 120 °C, respectively (Table 5, entries 2,3). The results clearly show the base role and NHC-ligand carbene property for TAIm[OH] and also show that TAIm[I] still has some basicity (refer to 12% yield in the absence of base, entry 1), but the formation of HI seems very difficult

and unlikely (according to the proposed mechanism). The catalytic activity of the TAIm[OH] (**3**)/Pd(OAc)₂ mixture was also studied in the presence and in the absence of K₃PO₄ as a base. As shown in Table 5, entries 4,5, the results in the presence and absence of K₃PO₄ did not differ and for both reactions 90% efficiency was obtained for 1 h. The results confirm well that there is no need for any external base in the coupling reactions.

In another experiment, two solvents, DMF and H₂O, were used instead of TAIm[OH], and no detectable efficiencies were observed for either (Table 5, entry 6). The results show that TAIm[OH], in addition to its high solubility, plays the role of ligand and base well. In another control test, the catalytic activity of **4** was evaluated towards Heck model reaction. The reaction afforded 85% of **12a** for 1 h; but the efficiency reached to 90% for 65 min (Table 5, entry 7). This slight difference may be directly related to the time required for the formation of the Pd complex in the mixture. In addition, the reaction can take place after the formation of the first species of palladium complex, which could be another reason for the slight difference in the catalytic activity of compound **4** with a mixture of **3**/Pd(OAc)₂. Also, this test clearly confirmed the base functionality for TAIm[OH] moiety.

3.5 Reusability

One of the main factor for a heterogeneous catalyst, which distinguishes it from the homogeneous type is its recyclability with the preservation of catalytic activity [33]. For a heterogeneous catalyst with magnetite solid support bearing immobilized metal complex, this factor is directly related to the metal leaching amount, stability during reaction medium, and deactivation. In this way, the heterogeneous nature of Fe₃O₄@SiO₂-TAIm[OH]-Pd was evaluated by three experiments of (i) hot filtration, (ii) mercury poisoning, and (iii)



Scheme 5 The three-phase test of 4-iodobenzene bounded Wang resin, *n*-butyl acrylate, and iodobenzene (in test 2) in the presence of $\text{Fe}_3\text{O}_4@ \text{SiO}_2\text{-TAIm}[\text{OH}]\text{-Pd}$

three-phase tests. All experiments were done on the Heck model reaction (Scheme 4) under optimized reaction conditions. For hot filtration test, the magnetic catalyst was filtered magnetically after 40 min of the reaction time with 38% conversion (based on GC analysis). The reaction was allowed to proceed for further 60 min. The coupling conversion reached to 40% after that time, which strongly confirmed the absence of any metal leaching to the mixture and heterogeneous performance of the catalyst. Mercury poisoning test was carried out by addition of 320 molar equivalents of $\text{Hg}(0)$ vs. Pd content after 40 min of the reaction time. The reaction mixture was stirred for another 60 min. The reaction conversion was determined by GC analysis and found to be 38%. $\text{Hg}(0)$ was adsorbed by metal sites on the catalyst surface (or by amalgamation) and deactivates the active sites and suppressed the catalytic activity immediately [29]. No progress in the reaction immediately after addition of $\text{Hg}(0)$ confirm this phenomena as well as the heterogeneous nature of the catalyst in agreement with the hot filtration test. Finally, the three-phase test, as a promising test for evaluation of a heterogeneous performance of a catalyst was applied over the catalyst (9) [29]. As shown in Scheme 5, a Wang resin-bound aryl iodide was reacted with *n*-butyl acrylate in water under reflux conditions in the presence of $\text{Fe}_3\text{O}_4@ \text{SiO}_2\text{-TAIm}[\text{OH}]\text{-Pd}$ (0.01 g, 0.2 mol% Pd). Didn't found any coupling product under these conditions, and at the end of the reaction, the catalyst was recovered magnetically. Moreover, the hydrolysis of the Wang resin by trifluoroacetic acid (TFAA) led to the formation of 4-iodobenzoic acid (Scheme 5, test 1). In another experiment, iodobenzene was also added to the mixture (Scheme 5, test 2). The experiment gives 87% conversion for 12 h for 95 min and no coupling product was detected after acid hydrolysis of the Wang resin. The results from the three-phase test clearly confirmed the heterogeneous nature and performance

of the catalyst for the C–C coupling reactions, completely in agreement with the hot filtration and $\text{Hg}(0)$ poisoning that suggest no considerable metal leaching occurs in the medium.

Finally, the recyclability of the heterogeneous catalyst (9) was evaluated over the Heck, Suzuki and Sonogashira cross-coupling reactions for the preparation of 12a, 14a, and 16a coupling products, respectively. All experiments were accomplished under optimized conditions (Tables 2–4). Figure 5a,d show the results of recycling and Pd metal leaching for the three coupling reactions. As evident in the figure, insignificant activity loss was observed for all the reactions, as 6%, 4%, and 5% loss in product isolated yield for Heck, Suzuki, and Sonogashira cross-coupling reactions respectively. Furthermore, didn't detect any Pd metal leaching by ICP analysis until cycle 4 for all coupling reactions in the residue (Fig. 5b). The leaching amount was slightly increased and reached to 2.5%, 1.8%, and 2.6% for Heck, Suzuki, and Sonogashira cross-coupling reactions respectively for 8th cycle. The recovered catalyst after 8th cycle was characterized by TEM analysis. As shown in Fig. 5c, a same morphology and particle size distribution was observed same as the corresponding freshly prepared catalyst. In addition, the oxidation state of Pd sites in the recovered catalyst was studied by high resolution XPS analysis. The results confirmed that the oxidation state of Pd active sites remained intact and consist of a mixture of 0 and +2 oxidation states (Fig. 5d). The results clearly confirmed the stability and high catalytic activity of the catalyst during the coupling reactions.

More importantly, the recyclability of TAIm[OH] was studied in each recycling. In this way, the model reaction of iodobenzene with styrene was chosen and in each cycle, EDX, density, and viscosity values were determined. The results were tabulated in Table 6. As shown in Table 6, the NHC ligand precursor retained its properties well in

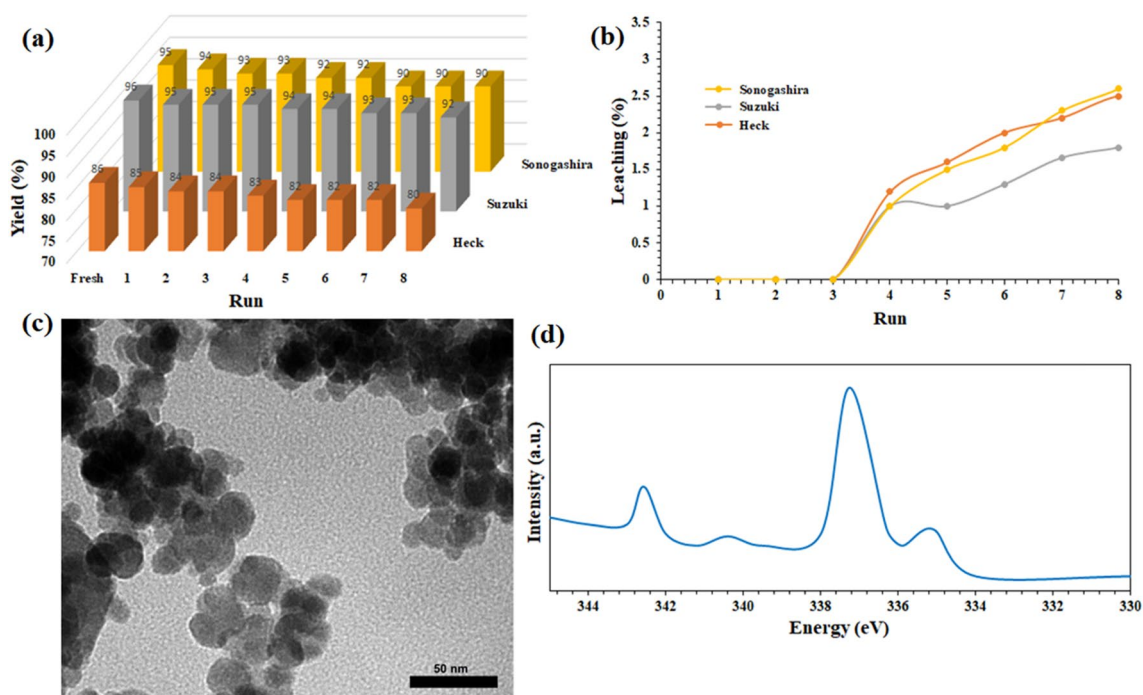


Fig. 5 **a** Recyclability and **b** leaching studies of catalyst **9** over the Heck (reaction of iodobenzene with styrene, preparation of **12a**), Suzuki (reaction of iodobenzene with phenylboronic acid, preparation of **14a**), and Sonogashira (reaction of iodobenzene with phenylacetylene, preparation of **16a**) coupling reactions under optimized condi-

tions. **c** TEM image and **d** high resolution XPS analysis (energy corrected) of the recovered catalyst **9** after 8th reaction cycle of Heck cross-coupling reaction of iodobenzene with styrene under optimized conditions

Table 6 Recyclability studies of TAlm[OH] over the reaction of iodobenzene with styrene

Physical properties	EDX elemental analysis (%wt)				Density (g.cm ⁻³) ^c	Viscosity (cP)	Yield (%)
	C	O	N	I ^b			
Fresh	49.33	35.76	14.91	0.00	1.52	1194	90
1 th cycle	49.47	35.52	14.95	0.06	1.52	1194	89
2 th cycle	49.62	35.25	15.05	0.08	1.52	1194	89
3 th cycle	49.76	34.96	15.18	0.10	1.54	1194	88
4 th cycle	49.90	34.80	15.16	0.14	1.53	1197	88
5 th cycle	50.05	34.55	15.18	0.22	1.57	1198	89
6 th cycle	50.22	34.20	15.28	0.30	1.57	1198	87
7 th cycle	50.39	33.94	15.33	0.34	1.57	1200	87
8 th cycle	50.52	33.68	15.36	0.44	1.58	1208	88

^aReaction conditions: Iodobenzene (1.0 mmol), styrene (1.3 mmol), H₂O (2.0 mL), Pd(OAc)₂ (1.0 mol%), recovered (except fresh) TAlm[OH] (2.0 mL), Ref., sealed tube, 60 min

^bIn this study, iodide was detected after 1th run due to the use of iodobenzene substrate

^cBased on apparatus. 1.55 g.cm⁻³ from the acid titration assay

successive cycles, which a very little efficiency loss per cycle (only 2% efficiency loss after the eighth cycle) was observed for the reaction. A very important result was the presence of iodide ions from the first cycle in the EDX analysis of the recovered TAlm[OH], which indicates that the structure of the catalyst is directly involved in the reaction. The presence of iodide increased slowly and increased

linearly from the fifth cycle onwards. As will be shown in the next section (Mechanistic Studies), the halide ion (from the aryl halide substrate) is replaced by the used HO⁻ ions in the reductive-elimination step. The presence of iodide is also responsible for the increase in density and viscosity, especially in the fifth and later cycles. However, under homogeneous and heterogeneous conditions, catalysts can

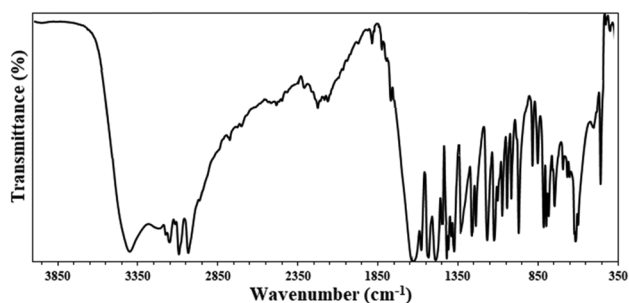


Fig. 6 FTIR spectrum of the recovered TAlm[OH] over the reaction of iodobenzene with styrene after 8th run

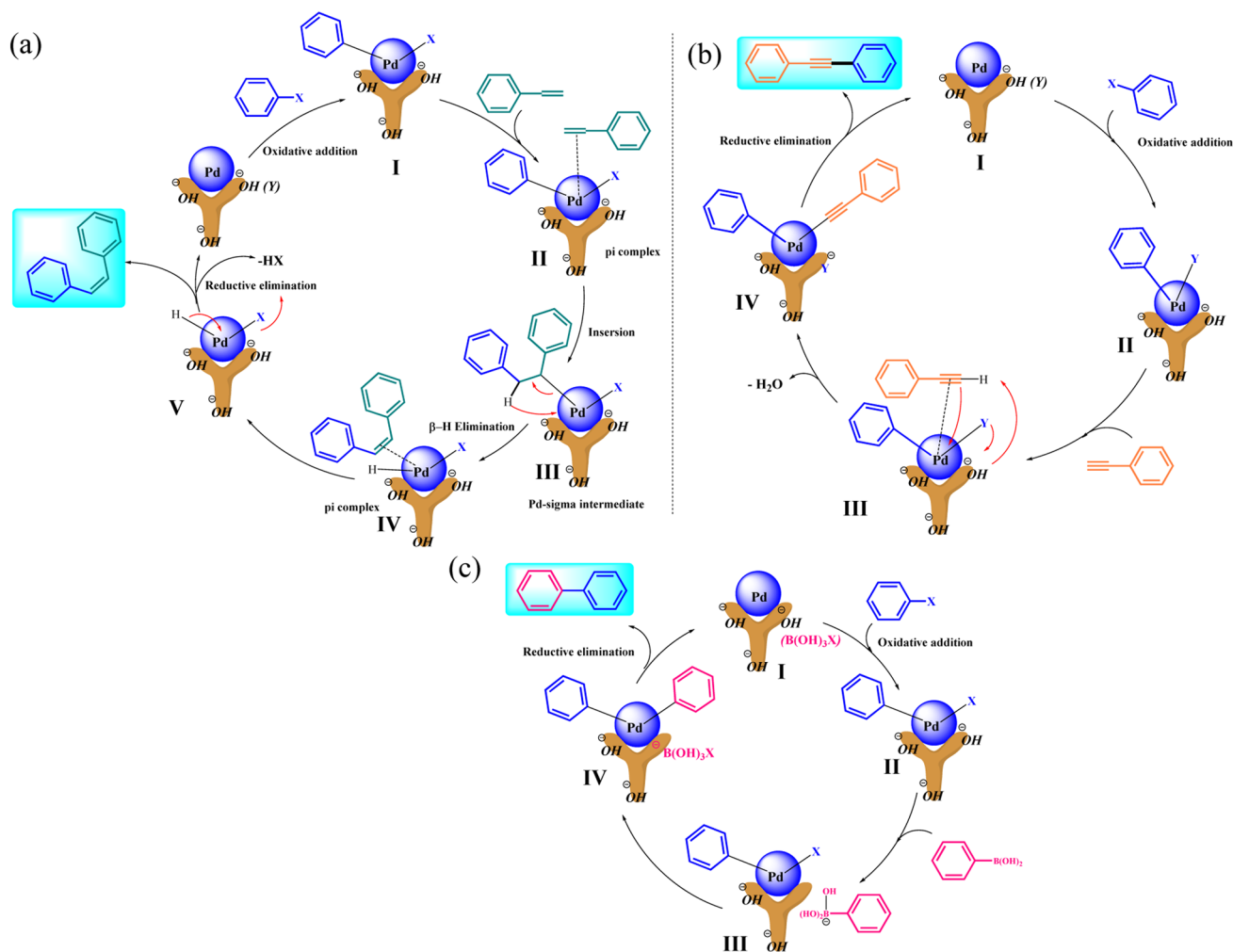
be used as long as there are hydroxide groups in the catalyst, or in other words, the catalyst is active.

In addition, FTIR spectrum of the recovered TAlm[OH] after 8th run confirmed preservation of the structure and

subsequently the stability of the NHC ligand precursor during consecutive recycles. As shown in Fig. 6, an almost identical FTIR spectrum than the freshly prepared was obtained for the recovered TAlm[OH].

3.6 Mechanism Studies

According to the obtained evidences and the mechanisms reported for Heck and Sonogashira reactions [34, 35], three mechanisms was proposed for the Heck, Sonogashira, and Suzuki coupling reactions catalyzed by $\text{Fe}_3\text{O}_4@ \text{SiO}_2\text{-TAlm[OH]-Pd}$ or TAlm[OH]-Pd. The results of XPS analysis showed that the coordinated Pd ions in TAlm[OH]-Pd have a mixture of 0 and +2 oxidation states. Therefore, according to the expectations and mechanisms reported for catalytic coupling reactions with Pd-based systems, the coupling reaction includes oxidative-addition and reductive-elimination steps. According to the proposed mechanism



Scheme 6 The proposed reaction mechanisms for $\text{Fe}_3\text{O}_4@ \text{SiO}_2\text{-TAlm[OH]-Pd}$ or TAlm[OH]-Pd catalyzed **a** Sonogashira, **b** Heck, and **c** Suzuki cross-coupling reactions

for Heck coupling reaction (Scheme 6a), the reaction initially begins with an oxidative-addition in the presence of aryl halide and the formation of the intermediate I. In the presence of an alkene, a π -complex II is formed and then an insertion is performed (Intermediate III). With a β -H elimination, a double bond is formed, followed by formation of a π -complex IV. The role of hydroxyl groups in the NHC ligand precursor as a base at this stage was proved by the tasks of: (i) reductive elimination, (ii) formation of the Heck product, and (iii) returns the catalyst to the cycle. The Sonogashira reaction is also performed according to the traditional mechanisms reported for the Pd-catalyzed Sonogashira reaction including oxidative-addition and reductive-elimination steps (Scheme 6b) [34–37].

As shown by the results obtained from the recovery of TAIM[OH] (Table 5, the presence and increase of iodine in successive cycles), the NHC ligand moiety promotes the reductive-elimination steps by absorbing the halide through its triazine framework. This result is also reflected in the mechanisms, and as shown in the schemes, the halide ion replaced by the used HO^- groups in the TAIM[OH] structure in the reductive-elimination step.

Subsequently, a similar mechanism was proposed for Suzuki cross-coupling according to the literature [34, 36]. The oxidation-addition reaction leads to the preparation of intermediate I (Scheme 6c). The basicity nature of the catalyst creates stable R-B(OH)_3^- -Cat. species (Int. II) in the presence of phenylboronic acid. The cationic nature of the catalyst ensures intermediate II stability. In the next step, the transmetalation leads to the bond formation of the aryl ring to the palladium sites and the removal of B(OH)_4^- . The reductive-elimination leads to the formation of the desired Suzuki product.

4 Conclusion

In this work, a new recyclable basic imidazolium ionic compound, TAIM[OH], has been synthesized and successfully characterized by FTIR, $^1\text{H-NMR}$, $^{13}\text{C-NMR}$, and EDX analyses. The NHC ligand precursor was prepared via the generation of three imidazolium [OH] functional groups on a triazine framework. The NHC ligand precursor was introduced by intrinsic properties including: density of 1.52 g.cm^{-3} , viscosity of 1194 cP , and Mw of 375.4 g.mol^{-1} . The activity of the NHC ligand precursor was evaluated for the base- and solvent-free Pd catalyzed C–C cross-coupling reactions of Heck, Suzuki and Sonogashira reactions as a homogeneous system. Another advantage of the work, was the ability of the Pd complex of NHC ligand precursor to immobilize

on magnetite with the preservation of its catalytic activity. The heterogeneous catalyst was also characterized by TGA, VSM, FE-SEM, TEM, XPS, EDX, and DLS analyses. However, the results revealed excellent catalytic activity for the both homogeneous and heterogeneous catalytic systems. The Pd sites in two catalytic systems were in a mixture of 0 and +2 oxidation states, which eliminates the need to any pre-activation or pre-reduction of Pd sites for an oxidative-addition and reductive elimination steps. The heterogeneous nature of the heterogeneous catalyst was confirmed by hot filtration, mercury (0) poisoning, and three-phase tests. Finally, the heterogeneous catalyst could be recycled for at least 8 consecutive runs for all three C–C coupling reactions with insignificant metal leaching and catalytic activity loss.

Supplementary Information The online version contains supplementary material available at <https://doi.org/10.1007/s10562-021-03552-5>.

Acknowledgement This work was sponsored in part by Natural Science Foundation of Liaoning Province (No. 20170520296).

Compliance with Ethical Standards

Conflict of interest There are no conflicts to declare.

References

- Cheng S, Wei W, Zhang X, Yu H, Huang M, Kazemnejadi M (2020) *Green Chem* 22:2069–2076
- Biajoli AF, Schwalm CS, Limberger J, Claudino TS, Monteiro AL (2014) *J Braz Chem Soc* 25:2186–2214
- Yousaf M, Zahoor AF, Akhtar R, Ahmad M, Naheed S (2019) *Mol Diversity* 24:821–839
- Asadi S, Sedghi R, Heravi MM (2017) *Catal Lett* 147:2045–2056
- Dalby A, Mo X, Stoa R, Wroblewski N, Zhang Z, Hagen TJ (2013) *Tetrahedron Lett* 54:2737–2739
- Thiel OR, Achmatowicz M, Milburn RM (2012) *Synlett* 23:1564–1574
- Liu C, Liu G, Zhao H (2016) *Chin J Chem* 34:1048–1052
- Sardarian AR, Kazemnejadi M, Esmailpour M (2019) *Dalton Trans* 48:3132–3145
- Tsoukala A, Bjørsvik H-R (2011) *Org Process Res Dev* 15:673–680
- Fu Y, Hong S, Li D, Liu S (2013) *J Agric Food Chem* 61:5347–5352
- Nishimura K, Kinugawa M (2012) *Org Process Res Dev* 16:225–231
- Rivara S, Piersanti G, Bartocchini F, Diamantini G, Pala D, Riccioni T, Stasi MA, Cabri W, Borsini F, Mor M, Tarzia G, Minetti P (2013) *J Med Chem* 56:1247–1261
- Chekal BP, Guinness SM, Lillie BM, McLaughlin RW, Palmer CW, Post RJ, Sieser JE, Singer RA, Sluggett GW, Vaidyanathan R, Withbroe GJ (2014) *Org Process Res Dev* 18:266–274
- Nasseri MA, Alavi SA, Kazemnejadi M, Allahresani A (2019) *RSC Adv* 9:20749–20759

15. Nasseri MA, Rezazadeh Z, Kazemnejadi M, Allahresani A (2019) *J Iran Chem Soc* 16:2693–2705
16. Sperry JB, Farr RM, Levent M, Ghosh M, Hoagland SM, Varso-lona RJ, Sutherland K (2012) *Org Process Res Dev* 16:1854–1860
17. Loubidi M, Moutardier A, Campos JF, Berteina-Raboin S (2018) *Tetrahedron Lett* 59:1050–1054
18. Zhang ZM, Xu B, Wu L, Wu Y, Qian Y, Zhou L, Liu Y, Zhang J (2019) *Angew Chem* 131:14795–14801
19. Yim JCH, Nambo M, Crudden CM (2017) *Org Lett* 19:3715–3718
20. Laffoon SD, Chan VS, Fickes MG, Kotecki B, Ickes AR, Henle J, Napolitano JG, Franczyk TS, Dunn TB, Barnes DM, Haight AR (2019) *ACS Catal* 9:11691–11708
21. Naeimi H, Kiani F (2018) *J Coord Chem* 71:1157–1167
22. Sadjadi S, Lazzara G, Malmir M, Heravi MM (2018) *J Catal* 366:245–257
23. Chen MT, Hsieh BY, Liu YH, Wu KH, Lussari N, Braga AA (2020). *Appl Organomet Chem*. <https://doi.org/10.1002/aoc.5870>
24. Ghotbinejad M, Khosropour AR, Mohammadpoor-Baltork I, Moghadam M, Tangestaninejad S, Mirkhani V (2014) *J Mol Catal A: Chem* 385:78–84
25. Wang T, Xu K, Wang W, Liu L (2018) *Transition Met Chem* 43:347–353
26. Aktaş A, Celepci DB, Gök Y (2019) *J Chem Sci* 131:78
27. Andrade GA, DiMeglio JL, Guardino ET, Yap GP, Rosenthal J (2017) *Polyhedron* 135:134–143
28. Wang X, Li S, Yu H, Yu J, Liu S (2011). *Chem–Eur J*. <https://doi.org/10.1002/chem.201101032>
29. Kazemnejadi M, Alavi SA, Rezazadeh Z, Nasseri MA, Allahresani A, Esmaeilpour M (2019) *Green Chem* 21:1718–1734
30. Nasseri MA, Alavi SA, Kazemnejadi M, Allahresani A (2019) *ChemistrySelect* 4:8493–8499
31. Long Y, Liang K, Niu J, Tong X, Yuan B, Ma J (2015) *New J Chem* 39:2988–2996
32. Veisi H, Najafi S, Hemmati S (2018) *Int J Biol Macromol* 113:186–194
33. Kazemnejadi M, Alavi SA, Rezazadeh Z, Nasseri MA, Allahresani A, Esmaeilpour M (2019) *J Mol Struct* 1186:230–249
34. Yang Q, Sane N, Klosowski D, Lee M, Rosenthal T, Wang NX, Wiensch E (2019) *Org Process Res Dev* 23:2148–2156
35. Brown RW, Zamani F, Gardiner MG, Yu H, Pyne SG, Hyland CJ (2019) *Chem Sci* 10:9051–9056
36. Li J, Yang S, Wu W, Jiang H (2018) *Eur J Org Chem* 2018:1284–1306
37. Christoffel F, Ward TR (2018) *Catal Lett* 148:489–511

Publisher's Note Springer Nature remains neutral with regard to jurisdictional claims in published maps and institutional affiliations.